2015 American Control Conference
Palmer House Hilton
July 1-3, 2015. Chicago, IL, USA

Moment-based Plant and String Stability Analysis of Connected Cruise Control with Stochastic Delays

Wubing B. Qin
Dept. of Mechanical Engineering
University of Michigan,
Ann Arbor, MI 48109, USA
Email: wubing@umich.edu

Marcella M. Gomez
Dept. of Biochemistry and Cell Biology
Rice University,
Houston, TX 77005, USA
Email: mg47@rice.edu

Gábor Orosz
Dept. of Mechanical Engineering
University of Michigan,
Ann Arbor, MI 48109, USA
Email: orosz@umich.edu

***Abstract*— In this paper we investigate the concept of connected cruise control (CCC) where vehicles rely on ad-hoc wireless vehicle-to-vehicle (V2V) communication to control their longitudinal motion. While V2V communication potentially allows vehicles to build detailed knowledge about the traffic environment, intermittencies and packet drops introduce stochastic delays into the communication channels that make control very challenging. We derive the mean and covariance dynamics for the corresponding stochastic system and analyze the effects of stochastic delays on vehicular strings. We also provide conditions for plant and string stability using the mean and the covariance. Moreover, we demonstrate that how the stable regimes shrink when the sampling time or the packet drop ratio increases. Our results have important implications regarding safety and efficiency of connected vehicle systems.**

I. Introduction

Emerging technologies in wireless vehicle-to-vehicle (V2V) communication may allow vehicles to obtain information about the motion of multiple vehicles ahead. This may lead to advanced longitudinal control algorithms, which can be implemented even when the vehicle is not equipped with additional sensors. We refer to this as connected cruise control (CCC) [1]. Apart from improving driver comfort and safety, the impact of CCC on traffic dynamics and mobility can be significant even for low penetration of CCC vehicles due to the long-range connections available [2,3]. However, for current dedicated short range communication (DSRC) devices, packets are usually broadcasted in every 100 ms [4], which requires the consideration of digital effects and time delays [5]. Moreover, packets may be dropped from time to time [6], which results in stochastic delay variations.

In this paper, we study the longitudinal dynamics of vehicles with stochastic delays in the communication channels and evaluate the stability of the uniform flow. In particular, we study plant stability, i.e., the ability of a CCC vehicle to follow a leader driving at a constant speed, and string stability, that is, the ability of a CCC vehicle to attenuate velocity fluctuations imposed by the leader. By analyzing the linearized system, we derive necessary conditions for plant and string stability of vehicular platoons using the mean dynamics, and necessary and sufficient conditions for plant and $n\sigma$ string stability using the covariance dynamics. Also, the performance degradations are evaluated when the packet delivery ratio decreases.

II. Preliminaries

In this paper, we need to use Kronecker product and vectorization of matrices intensively, so we recall the following definitions and theorems from [7].

Definition 1: Let $h_i \in \mathbb{R}^n$ denote the i-th column of the matrix $\mathbf{H} \in \mathbb{R}^{n\times m}$, i.e., $\mathbf{H} = [h_1 \quad h_2 \quad \dots \quad h_m]$. The vector operator $\overline{\text{vec}}(\mathbf{H}) \in \mathbb{R}^{mn}$ is defined as

$$\overline{\text{vec}}(\mathbf{H}) = \begin{bmatrix} h_1^{\mathrm{T}} & h_2^{\mathrm{T}} & \dots & h_m^{\mathrm{T}} \end{bmatrix}^{\mathrm{T}}. \tag{1}$$

Theorem 1: For matrices $\mathbf{A} \in \mathbb{R}^{m\times n}$, $\mathbf{B} \in \mathbb{R}^{n\times l}$, $\mathbf{C} \in \mathbb{R}^{p\times q}$ and $\mathbf{D} \in \mathbb{R}^{q\times r}$, we have

$$(\mathbf{AB}) \otimes (\mathbf{CD}) = (\mathbf{A} \otimes \mathbf{C})(\mathbf{B} \otimes \mathbf{D}), \tag{2}$$

where $\otimes$ denotes Kronecker product.

Theorem 2: For any three matrices $\mathbf{A}$, $\mathbf{B}$ and $\mathbf{C}$ for which the matrix product $\mathbf{ABC}$ is defined, we have

$$\overline{\text{vec}}(\mathbf{ABC}) = (\mathbf{C}^{\mathrm{T}} \otimes \mathbf{A})\overline{\text{vec}}(\mathbf{B}). \tag{3}$$

Definition 2: For a random variable $\boldsymbol{x} \in \mathbb{R}^n$, the second moment and the second central moment are defined as $\mathbb{E}[\boldsymbol{x} \otimes \boldsymbol{x}]$ and $\mathbb{E}[(\boldsymbol{x}-\boldsymbol{\mu}) \otimes (\boldsymbol{x}-\boldsymbol{\mu})]$, respectively, where $\boldsymbol{\mu} = \mathbb{E}[\boldsymbol{x}]$ denotes the mean. It can be shown that

$$\mathbb{E}[(\boldsymbol{x}-\boldsymbol{\mu}) \otimes (\boldsymbol{x}-\boldsymbol{\mu})] = \overline{\text{vec}}\big(\mathbb{E}[(\boldsymbol{x}-\boldsymbol{\mu})(\boldsymbol{x}-\boldsymbol{\mu})^{\mathrm{T}}]\big), \tag{4}$$

where $\mathbb{E}[(\boldsymbol{x}-\boldsymbol{\mu})(\boldsymbol{x}-\boldsymbol{\mu})^{\mathrm{T}}]$ is the covariance matrix.

III. Connected Cruise Control with Stochastic Delays

In this section, we present a CCC design while incorporating stochastic delay variations due to the packet loss in wireless V2V communication. Fig. 1 shows a vehicle chain where each vehicle is using the information received from the vehicle immediately ahead via wireless communication. This can be viewed as the concatenation of leader-follower pairs. We consider a nonlinear controller that acts on the inter-vehicle distance (or headway) h, which can be calculated from GPS coordinates, the leader's velocity v_{L}, and the vehicle's own velocity v.

The leader broadcasts its kinematic information intermittently with a sampling time of Δt, which yields the time

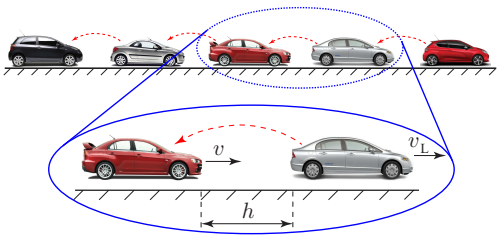

Fig. 1. The top row shows a chain of vehicles equipped with V2V communication on a single lane, which is the concatenation of leader-follower configuration displayed at the bottom. Dashed arrows indicate wireless communication links between vehicles.

mesh $t_k = k\Delta t$ for $k = 0, 1, 2, \ldots$; see Fig. 2(a). According to the IEEE802.11p protocol used in DSRC, the transmitter is unaware whether the broadcasted packet has been successfully delivered and no packets are re-transmitted. We assume that at time instant t_k, previous $\tau(k)-1$ packets have been dropped consecutively. Thus, the last packet received successfully was transmitted at time instant $t_{k-\tau(k)}$. The controller outputs a command based on this information at $t_{k-\tau(k)+1}$, that is kept constant until t_{k+1} using a zero-order hold, since no new packet is delivered successfully until t_k; see Fig. 2(b). Since the packet drop dynamics is governed by a stochastic process, the digitally controlled system is forced by piecewise constant inputs of stochastically varying length. Fig. 2(d) shows the time evolution of $\tau(k)$, which can be formulated as

$$\tau(k+1) = \begin{cases} 1, & \text{if a packet is received} \\ & \text{during } [t_k,\, t_{k+1}), \\ \tau(k)+1, & \text{otherwise.} \end{cases} \tag{5}$$

Assuming that the packet delivery ratio is q, the probability density function of $\tau(k)$ is given by the geometric distribution

$$f_{\tau(k)}(\xi) = \textstyle\sum_{r=1}^{\infty} w_r \delta(\xi - r) \quad \text{with} \quad \sum_{r=1}^{\infty} w_r = 1\,, \tag{6}$$

where $\delta(*)$ denotes the Dirac delta function and

$$w_r = q(1-q)^{r-1}, \tag{7}$$

see [6]. In order to avoid infinitely large delays, we truncate the distribution such that

$$w_r = \begin{cases} q(1-q)^{r-1} & \text{if} \quad r = 1\,,\, \ldots\,,\, N-1\,, \\ 1 - \sum_{i=1}^{N-1} w_i = (1-q)^{N-1} & \text{if} \quad r = N\,, \\ 0 & \text{if} \quad r > N\,, \end{cases} \tag{8}$$

i.e., $\tau(k+1) = 1$ if $\tau(k) = N$, where N is the maximum number of trials. We choose N such that $\sum_{r=1}^{N-1} w_r \geq p_{\rm cr}$ holds where $p_{\rm cr}$ is the critical cumulative delivery ratio. For example, based on the worst case scenario $q = 0.58$ presented in [6], using $p_{\rm cr} = 0.99$ the maximum value is $N = 6$.

Notice that since the dynamics of the vehicle still evolve in continuous time, the corresponding effective delay increases from $\tau(k)\Delta t$ to $\big(\tau(k)+1\big)\Delta t$ linearly during each sampling interval. Such stochastic delay variations are shown in Fig. 2(c).

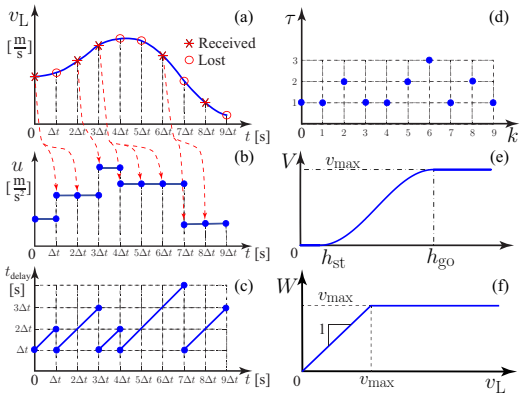

Fig. 2. (a) Leader's velocity is transmitted every Δt time, but packets may be dropped as indicated. (b) Controller output while using ZOH based on the newest received information. (c) Time-delay variations arising in system (9,10). (d) Time-delay variations arising in the corresponding discrete-time system (15). (e) Range policy function (11). (f) Saturation function (12).

For simplicity we consider zero inclination and omit rolling resistance and air drag effects in the physics-based model [1], which leads to the simplified vehicle dynamics

$$\begin{aligned} \dot{h}(t) &= v_{\rm L}(t) - v(t)\,, \\ \dot{v}(t) &= u(t_{k-\tau(k)})\,, \end{aligned} \tag{9}$$

for $t_k \leq t < t_{k+1}$. We choose the nonlinear controller

$$u(t) = K_{\rm p}\Big(V\big(h(t)\big) - v(t)\Big) + K_{\rm v}\Big(W\big(v_{\rm L}(t)\big) - v(t)\Big)\,, \tag{10}$$

cf. [5]. The linearized version of this is widely used in the literature [8,9,10,11,12].

The range policy $V(h)$ gives the desired velocity as a function of the headway h, and must be

- continuous and monotonously increasing (the more sparse traffic is, the faster the vehicles intend to run);
- zero for $h \leq h_{\rm st}$ (vehicles intend to stop within a safety distance);
- maximal for $h \geq h_{\rm go}$ (vehicles intend to run as fast as they can in sparse traffic – often referred to as free flow).

In this paper, we choose the continuously differentiable range policy

$$V(h) = \begin{cases} 0 & \text{if} \quad h \leq h_{\rm st}\,, \\ \dfrac{v_{\max}}{2}\Big(1 - \cos\big(\pi \frac{h - h_{\rm st}}{h_{\rm go} - h_{\rm st}}\big)\Big) & \text{if} \quad h_{\rm st} < h < h_{\rm go}\,, \\ v_{\max} & \text{if} \quad h \geq h_{\rm go}\,, \end{cases} \tag{11}$$

shown in Fig. 2(e). Moreover, the saturation function $W(v_{\rm L})$ describes the switching between CCC mode ($v_{\rm L} \leq v_{\max}$) and normal cruise control mode ($v_{\rm L} > v_{\max}$) such that

$$W(v_{\rm L}) = \begin{cases} v_{\rm L} & \text{if} \quad v_{\rm L} \leq v_{\max}\,, \\ v_{\max} & \text{if} \quad v_{\rm L} > v_{\max}\,, \end{cases} \tag{12}$$

see Fig. 2(f).

For $v_{\rm L} \leq v_{\max}$ (CCC mode), system (9,10) possesses the equilibrium

$$v_{\rm L}^* = v^* = V(h^*)\,. \tag{13}$$

Our goal is to design the control gains $K_{\rm p}$, $K_{\rm v}$ to ensure that the system can reach this equilibrium (i.e., plant stability is satisfied) and also attenuate perturbations introduced by the leader (i.e., string stability holds) in the presence of stochastic delay variations.

IV. Discretization and Linearization

Fourier's theory states that periodic signals can be represented as an infinite sum of sines and cosines, which can also be extended to absolutely integrable non-periodic signals. Henceforth, we will assume sinusoidal variations of the leader's velocity. Solving the differential equation (9,10) with input

$$v_{\rm L}(t) = v_{\rm L}^* + v_{\rm L}^{\rm amp}\sin(\omega t) \tag{14}$$

along the time interval $[t_k,\, t_{k+1})$ in CCC mode, one may derive the discrete-time nonlinear map

$$\begin{aligned}\begin{bmatrix} h(t_{k+1}) \\ v(t_{k+1}) \end{bmatrix} &= \begin{bmatrix} 1 & -\Delta t \\ 0 & 1 \end{bmatrix}\begin{bmatrix} h(t_k) \\ v(t_k) \end{bmatrix} \\ &+ \begin{bmatrix} \alpha_1 & \alpha_2 \\ 0 & 0 \end{bmatrix}\begin{bmatrix} v_{\rm L}(t_k) - v_{\rm L}^* \\ v_{\rm L}^{\perp}(t_k) - v_{\rm L}^* \end{bmatrix} \\ &+ \begin{bmatrix} 0 & \frac{1}{2}\Delta t^2(K_{\rm p}+K_{\rm v}) \\ 0 & -\Delta t(K_{\rm p}+K_{\rm v}) \end{bmatrix}\begin{bmatrix} h\big(t_{k-\tau(k)}\big) \\ v\big(t_{k-\tau(k)}\big) \end{bmatrix} \\ &+ \begin{bmatrix} -\frac{1}{2}\Delta t^2 K_{\rm v} & 0 \\ \Delta t K_{\rm v} & 0 \end{bmatrix}\begin{bmatrix} v_{\rm L}\big(t_{k-\tau(k)}\big) \\ v_{\rm L}^{\perp}\big(t_{k-\tau(k)}\big) \end{bmatrix} \\ &+ \begin{bmatrix} -\frac{1}{2}\Delta t^2 K_{\rm p} \\ \Delta t K_{\rm p} \end{bmatrix} V\Big(h\big(t_{k-\tau(k)}\big)\Big) + \begin{bmatrix} v^*\Delta t \\ 0 \end{bmatrix}, \end{aligned} \tag{15}$$

where

$$\begin{aligned} v_{\rm L}^{\perp}(t) &= v_{\rm L}^* + v_{\rm L}^{\rm amp}\cos(\omega t), \\ \alpha_1 &= \frac{\sin(\omega\Delta t)}{\omega}, \quad \alpha_2 = \frac{1-\cos(\omega\Delta t)}{\omega}. \end{aligned} \tag{16}$$

That is, in the discrete-time system (15), $\tau(k)$ plays the role of a discrete stochastic delay, see Fig. 2(d). Notice that the scalar sinusoidal input (14) that drives the continuous-time system (9) results in the vector-valued input for the discrete-time system (15).

Then we linearize the system about the equilibrium (13). Defining the perturbations $\tilde{h}(t) = h(t) - h^*$, $\tilde{v}(t) = v(t) - v^*$, $\tilde{v}_{\rm L}(t) = v_{\rm L}(t) - v_{\rm L}^*$, $\tilde{v}_{\rm L}^{\perp}(t) = v_{\rm L}^{\perp}(t) - v_{\rm L}^*$, we obtain

$$\begin{aligned} X(k+1) &= \mathbf{A}\,X(k) + \mathbf{B}\,U(k) \\ &\quad + \mathbf{A}_\tau\,X\big(k-\tau(k)\big) + \mathbf{B}_\tau\,U\big(k-\tau(k)\big), \\ Y(k) &= \mathbf{C}\,X(k), \end{aligned} \tag{17}$$

where the state, the input and the output are defined as

$$X(k) = \begin{bmatrix} \tilde{h}(t_k) \\ \tilde{v}(t_k) \end{bmatrix},\; U(k) = \begin{bmatrix} \tilde{v}_{\rm L}(t_k) \\ \tilde{v}_{\rm L}^{\perp}(t_k) \end{bmatrix},\; Y(k) = \tilde{v}(t_k), \tag{18}$$

and the matrices are given by

$$\begin{aligned} \mathbf{A} &= \begin{bmatrix} 1 & -\Delta t \\ 0 & 1 \end{bmatrix}, \quad \mathbf{B} = \begin{bmatrix} \alpha_1 & \alpha_2 \\ 0 & 0 \end{bmatrix}, \\ \mathbf{A}_\tau &= \begin{bmatrix} -\frac{1}{2}\Delta t^2 K_{\rm p} N_* & \frac{1}{2}\Delta t^2(K_{\rm p}+K_{\rm v}) \\ \Delta t K_{\rm p} N_* & -\Delta t(K_{\rm p}+K_{\rm v}) \end{bmatrix}, \\ \mathbf{B}_\tau &= \begin{bmatrix} -\frac{1}{2}\Delta t^2 K_{\rm v} & 0 \\ \Delta t K_{\rm v} & 0 \end{bmatrix}, \quad \mathbf{C} = \begin{bmatrix} 0 & 1 \end{bmatrix}, \end{aligned} \tag{19}$$

where

$$\begin{aligned} N_* &= V'(h^*) = V'\big(V^{-1}(v^*)\big) \\ &= \begin{cases} \dfrac{\pi\sqrt{v^*(v_{\max}-v^*)}}{h_{\rm go}-h_{\rm st}} & \text{if} \quad h_{\rm st} < h < h_{\rm go}, \\ 0 & \text{elsewhere}, \end{cases} \end{aligned} \tag{20}$$

cf. (11). Also, notice that

$$U(k-r) = \mathbf{R}^r\,U(k), \tag{21}$$

where

$$\mathbf{R} = \begin{bmatrix} \cos(\omega\Delta t) & -\sin(\omega\Delta t) \\ \sin(\omega\Delta t) & \cos(\omega\Delta t) \end{bmatrix}. \tag{22}$$

Defining the $2(N+1)$-dimensional augmented state

$$\hat{X}(k) = \begin{bmatrix} X(k) \\ X(k-1) \\ \vdots \\ X(k-N) \end{bmatrix}, \tag{23}$$

(17) can be written as

$$\begin{aligned} \hat{X}(k+1) &= \hat{\mathbf{A}}_{\tau(k)}\,\hat{X}(k) + \hat{\mathbf{B}}_{\tau(k)}\,U(k), \\ Y(k) &= \hat{\mathbf{C}}\,\hat{X}(k), \end{aligned} \tag{24}$$

where $\hat{\mathbf{A}}_{\tau(k)} \in \mathbb{R}^{2(N+1)\times 2(N+1)}$ and $\hat{\mathbf{B}}_{\tau(k)} \in \mathbb{R}^{2(N+1)\times 2}$ can take the values

$$\begin{aligned} \hat{\mathbf{A}}_r &= \begin{bmatrix} \mathbf{A} & \delta_{1r}\,\mathbf{A}_\tau & \delta_{2r}\,\mathbf{A}_\tau & \cdots & \delta_{Nr}\,\mathbf{A}_\tau \\ \mathbf{I} & \mathbf{0} & \mathbf{0} & \cdots & \mathbf{0} \\ \mathbf{0} & \mathbf{I} & \mathbf{0} & \cdots & \mathbf{0} \\ \vdots & \ddots & \ddots & \ddots & \vdots \\ \mathbf{0} & \cdots & \mathbf{0} & \mathbf{I} & \mathbf{0} \end{bmatrix}, \\ \hat{\mathbf{B}}_r &= \begin{bmatrix} \mathbf{B} + \mathbf{B}_\tau\,\mathbf{R}^r \\ \mathbf{0} \\ \vdots \\ \mathbf{0} \end{bmatrix}, \end{aligned} \tag{25}$$

for $r = 1, \ldots, N$, cf. (19). Here, δ_{ir} denotes the Kronecker delta, while $\mathbf{I} \in \mathbb{R}^{2\times 2}$ and $\mathbf{0} \in \mathbb{R}^{2\times 2}$ denote identity and zero matrices, respectively. Also we have

$$\hat{\mathbf{C}} = \begin{bmatrix} \mathbf{C} & \mathbf{0}' & \cdots & \mathbf{0}' \end{bmatrix}, \tag{26}$$

where $\hat{\mathbf{C}} \in \mathbb{R}^{1\times 2(N+1)}$, and $\mathbf{0}' = \begin{bmatrix} 0 & 0 \end{bmatrix}$.

Note that in (24), $\hat{\mathbf{A}}_{\tau(k)}$ depends on $\hat{\mathbf{A}}_{\tau(k-1)}$ according to (5,6,8), which also holds for $\hat{\mathbf{B}}_{\tau(k)}$ and $\hat{\mathbf{B}}_{\tau(k-1)}$, implying that (24) is a non-Markovian stochastic process. However, to simplify the analysis, we assume that $\tau(k)$ is independently identically distributed (i.i.d.) with the probability density function (6,8).

V. Mean and Covariance Dynamics

In this section, the dynamics for the mean and covariance will be derived. Let us define the deterministic variables

$$\bar{X}(k) = \mathbb{E}[\hat{X}(k)], \;\; \bar{Y}(k) = \mathbb{E}[\hat{Y}(k)]. \tag{27}$$

By taking expectations of both sides of (24), one can derive the equation describing the mean dynamics

$$\begin{aligned} \bar{X}(k+1) &= \bar{\mathbf{A}}\,\bar{X}(k) + \bar{\mathbf{B}}\,U(k)\,, \\ \bar{Y}(k) &= \bar{\mathbf{C}}\,\bar{X}(k)\,, \end{aligned} \tag{28}$$

where

$$\bar{\mathbf{A}} = \textstyle\sum_{r=1}^{N} w_r \hat{\mathbf{A}}_r\,, \quad \bar{\mathbf{B}} = \sum_{r=1}^{N} w_r \hat{\mathbf{B}}_r\,, \quad \bar{\mathbf{C}} = \hat{\mathbf{C}}. \tag{29}$$

Then the covariance is defined as

$$\begin{aligned} \bar{\bar{X}}(k) &= \mathbb{E}\big[\big(\hat{X}(k) - \bar{X}(k)\big) \otimes \big(\hat{X}(k) - \bar{X}(k)\big)\big]\,, \\ \bar{\bar{Y}}(k) &= \mathbb{E}\big[\big(\hat{Y}(k) - \bar{Y}(k)\big) \otimes \big(\hat{Y}(k) - \bar{Y}(k)\big)\big]\,, \end{aligned} \tag{30}$$

and it can be shown that

$$\begin{aligned} \bar{\bar{X}}(k) &= \mathbb{E}[\hat{X}(k) \otimes \hat{X}(k)] - \bar{X}(k) \otimes \bar{X}(k)\,, \\ \bar{\bar{Y}}(k) &= \mathbb{E}[\hat{Y}(k) \otimes \hat{Y}(k)] - \bar{Y}(k) \otimes \bar{Y}(k)\,. \end{aligned} \tag{31}$$

Thus, using (24), one can obtain the covariance dynamics

$$\begin{aligned} \bar{\bar{X}}(k+1) &= \bar{\bar{\mathbf{A}}}\bar{\bar{X}}(k) \\ &\quad + \bar{\bar{\mathbf{H}}}_1\big(\bar{X}(k) \otimes \bar{X}(k)\big) + \bar{\bar{\mathbf{H}}}_2\big(\bar{X}(k) \otimes U(k)\big) \\ &\quad + \bar{\bar{\mathbf{H}}}_3\big(U(k) \otimes \bar{X}(k)\big) + \bar{\bar{\mathbf{H}}}_4\big(U(k) \otimes U(k)\big)\,, \\ \bar{\bar{Y}}(k) &= \bar{\bar{\mathbf{C}}}\bar{\bar{X}}(k)\,, \end{aligned} \tag{32}$$

where

$$\begin{aligned} \bar{\bar{\mathbf{A}}} &= \textstyle\sum_{r=1}^{N} w_r \hat{\mathbf{A}}_r \otimes \hat{\mathbf{A}}_r\,, \\ \bar{\bar{\mathbf{H}}}_1 &= \textstyle\sum_{r=1}^{N} w_r \hat{\mathbf{A}}_r \otimes \hat{\mathbf{A}}_r - \bar{\mathbf{A}} \otimes \bar{\mathbf{A}}\,, \\ \bar{\bar{\mathbf{H}}}_2 &= \textstyle\sum_{r=1}^{N} w_r \hat{\mathbf{A}}_r \otimes \hat{\mathbf{B}}_r - \bar{\mathbf{A}} \otimes \bar{\mathbf{B}}\,, \\ \bar{\bar{\mathbf{H}}}_3 &= \textstyle\sum_{r=1}^{N} w_r \hat{\mathbf{B}}_r \otimes \hat{\mathbf{A}}_r - \bar{\mathbf{B}} \otimes \bar{\mathbf{A}}\,, \\ \bar{\bar{\mathbf{H}}}_4 &= \textstyle\sum_{r=1}^{N} w_r \hat{\mathbf{B}}_r \otimes \hat{\mathbf{B}}_r - \bar{\mathbf{B}} \otimes \bar{\mathbf{B}}\,, \\ \bar{\bar{\mathbf{C}}} &= \hat{\mathbf{C}} \otimes \hat{\mathbf{C}}\,. \end{aligned} \tag{33}$$

To simplify (32), first we assume that the mean dynamics is stable and already at steady state. When the mean dynamics is plant stable, the transient response will converge to zero, and the steady state response will share the same form with the input, i.e., it is a sinusoidal signal. Thus, at steady state, one can assume

$$\bar{X}(k) = \mathbf{Q}U(k)\,. \tag{34}$$

Substituting (34) into (28) and using (21), one can get

$$\mathbf{Q} - \bar{\mathbf{A}}\mathbf{Q}\mathbf{R} = \bar{\mathbf{B}}\mathbf{R}\,. \tag{35}$$

Thus, $\mathbf{Q}$ can be obatined by solving

$$(\mathbf{I} \otimes \bar{\mathbf{I}} - \mathbf{R}^{\mathrm{T}} \otimes \bar{\mathbf{A}})\overline{\mathrm{vec}}(\mathbf{Q}) = \overline{\mathrm{vec}}(\bar{\mathbf{B}}\mathbf{R})\,. \tag{36}$$

cf. (3). Considering (34), the covariance dynamics (32) becomes

$$\begin{aligned} \bar{\bar{X}}(k+1) &= \bar{\bar{\mathbf{A}}}\bar{\bar{X}}(k) + \bar{\bar{\mathbf{B}}}\bar{\bar{U}}(k)\,, \\ \bar{\bar{Y}}(k) &= \bar{\bar{\mathbf{C}}}\bar{\bar{X}}(k)\,, \end{aligned} \tag{37}$$

where

$$\bar{\bar{U}}(k) = U(k) \otimes U(k)\,, \tag{38}$$

$\bar{\bar{\mathbf{A}}}$ and $\bar{\bar{\mathbf{C}}}$ are given in (33) while

$$\begin{aligned} \bar{\bar{\mathbf{B}}} &= \textstyle\sum_{r=1}^{N} w_r\big(\hat{\mathbf{A}}_r\mathbf{Q} + \hat{\mathbf{B}}_r\big) \otimes \big(\hat{\mathbf{A}}_r\mathbf{Q} + \hat{\mathbf{B}}_r\big) \\ &\quad - \big(\bar{\mathbf{A}}\mathbf{Q} + \bar{\mathbf{B}}\big) \otimes \big(\bar{\mathbf{A}}\mathbf{Q} + \bar{\mathbf{B}}\big)\,. \end{aligned} \tag{39}$$

VI. Plant Stability Analysis

Plant stability means that the follower is capable of approaching the leader's velocity when the leader is driving at a constant velocity. In this section, plant stability for both the mean dynamics (28) and covariance dynamics (37) are given, where plant stability of the mean dynamics gives the necessary condition for the plant stability of the stochastic system (24). On the other hand, plant stability of the covariance dynamics provides the necessary and sufficient condition for the plant stability of the stochastic system (24).

For plant stability of the mean dynamics, all the eigenvalues of the corresponding system matrix $\bar{\mathbf{A}}$ in (28) must lie within the unit circle in the complex plane. The eigenvalues $z \in \mathbb{C}$ are given by the characteristic equation

$$\det(z\,\bar{\mathbf{I}} - \bar{\mathbf{A}}) = 0\,, \tag{40}$$

where $\bar{\mathbf{I}} \in \mathbb{R}^{2(N+1)\times 2(N+1)}$ is the identity matrix. There are three different ways where the system can lose stability [13].

(i) One real eigenvalue crosses the unit circle at 1;

(ii) One real eigenvalue crosses the unit circle at -1;

(iii) A pair of complex conjugate eigenvalues crosses the unit circle at $\mathrm{e}^{\pm \mathrm{j}\theta}$.

By substituting the critical eigenvalue(s) into the characteristic equation (40), one can obtain the stability boundaries represented in the parameter space $(K_{\mathrm{p}}, K_{\mathrm{v}}, v^*, w, \Delta t)$, where w denotes the set of all the w_r-s for $r \in \{1, 2, \ldots, N\}$. In case (iii), one needs to separate the real and imaginary parts and equate them to zero in order to obtain the stability boundary parameterized by θ.

For plant stability of the covariance dynamics, all the eigenvalues of the corresponding system matrix $\bar{\bar{\mathbf{A}}}$ in (37) must lie within the unit circle in the complex plane. Here, the eigenvalues $z \in \mathbb{C}$ are given by the characteristic equation

$$\det(z\,\bar{\bar{\mathbf{I}}} - \bar{\bar{\mathbf{A}}}) = 0\,, \tag{41}$$

where $\bar{\bar{\mathbf{I}}} \in \mathbb{R}^{2^2(N+1)^2 \times 2^2(N+1)^2}$ is the identity matrix. Similar to plant stability for the mean dynamics, the corresponding stability boundaries can be obtained for three different kinds of stability losses.

Fig. 3 shows the stability charts in the $(K_{\mathrm{v}}, K_{\mathrm{p}})$-plane for different values of the packet delivery ratio q and sampling time Δt. The inlets show the probability distribution of discrete stochastic delay given by (6). The horizontal red line and the red curves represent plant stability boundaries for the mean dynamics (28), and the region enclosed by these curves, i.e., the union of all shaded regions, are mean plant stable. Solid purple curves represent plant stability boundaries for the covariance dynamics (37), and the the region enclosed by them are covariance plant stable. (The green and blue curves and the corresponding lobe-shaped regions will be explained in Section VII.) Both the mean and covariance plant stable domains shrink as the packet delivery ratio q decreases and as sampling ratio Δt increases. For the mean dynamics (28), the arising oscillation frequency is zero along the horizontal red line while the frequency increases monotonously along the red curve, that is, the further we are

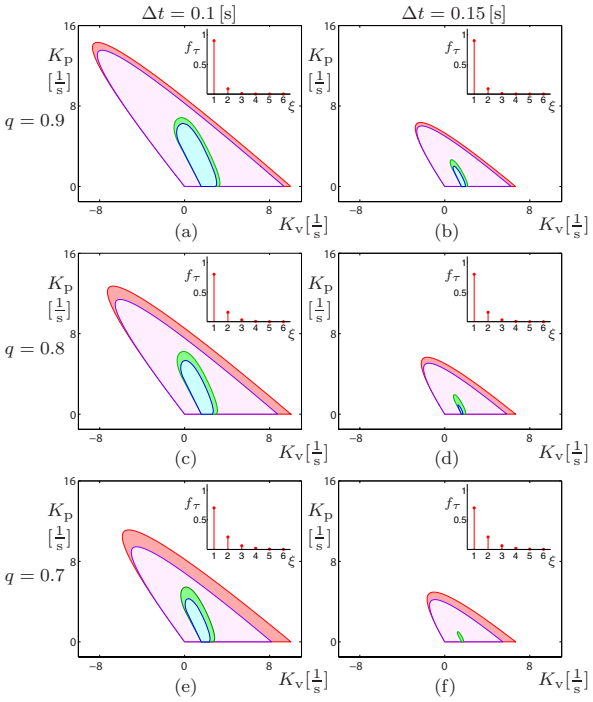

Fig. 3. Stability diagrams in the $(K_\mathrm{v}, K_\mathrm{p})$-plane for $v_\mathrm{max} = 30\,\mathrm{m/s}$, $h_\mathrm{st} = 5\,\mathrm{m}$, $h_\mathrm{go} = 35\,\mathrm{m}$, $v^* = 15\,\mathrm{m/s}$ (cf. (11,13)) and different values of packet delivery ratio q and sampling time Δt as indicated. The corresponding delay distributions (6) are plotted on each panel as inlets. Red and green curves correspond to changes in plant and string stability of the mean dynamics (28), respectively, and purple and blue curves correspond to changes in plant and 1σ string stability of the covariance dynamics (37), respectively.

from the origin (along the curve), the higher the frequency of the arising oscillation is. However, for the covariance dynamics, the oscillation frequency is zero along both the horizontal purple line and the purple curve, implying that the covariance always loses plant stability without oscillations.

VII. String Stability Analysis

String stability means that the follower is capable of attenuating fluctuations in the leader's velocity. For linear systems, string stability is equivalent to the attenuation of sinusoidal signals at all frequencies [14]. In this section, string stability for both the mean dynamics (28) and covariance dynamics (37) are given. String stability for the mean dynamics gives necessary condition for the string stability of the stochastic system (24) while the covariance dynamics is used to determine the $n\sigma$-string stability.

For string stability of the mean dynamics, we consider $\tilde{v}(t)$ as output corresponding to periodic input (14). After discretizing time (cf. (17,18)), we obtain two discrete inputs $\tilde{v}_\mathrm{L}(t_k) = \tilde{v}_\mathrm{L}(k)$ and $\tilde{v}_\mathrm{L}^\perp(t_k) = \tilde{v}_\mathrm{L}^\perp(k)$, and one discrete output $\tilde{v}(t_k) = \tilde{v}(k)$. However, the inputs are not linearly independent, so their effects have to be summed up. Applying Z-transform to (28), one can obtain the corresponding transfer function

$$\bar{\Gamma}(z) := [\bar{\gamma}_1(z) \quad \bar{\gamma}_2(z)] = \bar{\mathbf{C}}\big(z\,\bar{\mathbf{I}} - \bar{\mathbf{A}}\big)^{-1}\bar{\mathbf{B}}. \tag{42}$$

Following the same method as in [15], one can get the steady state output

$$\bar{Y}_\mathrm{ss}(k) = \bar{M}(\omega) v_\mathrm{L}^\mathrm{amp} \sin\big(k\omega\Delta t + \bar{\psi}(\omega)\big), \tag{43}$$

where

$$\bar{M}(\omega) = \sqrt{|\bar{\gamma}_1|^2 + |\bar{\gamma}_2|^2 + 2\mathrm{Im}(\bar{\gamma}_1\bar{\gamma}_2^*)}\,, \tag{44}$$

is the amplification ratio, $\bar{\psi}(\omega)$ is the phase lag at frequency ω, and $*$ denotes the complex conjugate.

Then the string stability boundaries in the parameter space are given by

$$\begin{cases} \bar{M}(\bar{\omega}_\mathrm{cr}) = 1, \\ \bar{M}'(\bar{\omega}_\mathrm{cr}) = 0, \end{cases} \tag{45}$$

for critical excitation frequency $\bar{\omega}_\mathrm{cr} > 0$, where prime denotes differentiation with respect to ω. Note that $\bar{M}$ also depends on the parameters $(K_\mathrm{p}, K_\mathrm{v}, w, v^*, \Delta t)$. Finally, one may show that $\bar{M}(0) = 1, \bar{M}'(0) = 0$ always holds. Therefore, the string stability boundary at $\bar{\omega}_\mathrm{cr} = 0$ is given by

$$\bar{M}''(0) = 0. \tag{46}$$

For string stability of the covariance dynamics, from (38), one may notice that the input $\bar{\bar{U}}(k)$ can be separated into a constant part and a harmonic excitation part, i.e.

$$\bar{\bar{U}}(k) = \bar{\bar{U}}_0 + \bar{\bar{U}}_1(k)\,, \tag{47}$$

where

$$\bar{\bar{U}}_0 = \frac{1}{2}\big(v_\mathrm{L}^\mathrm{amp}\big)^2 \bar{\bar{u}}_0\,, \quad \bar{\bar{U}}_1(k) = \frac{1}{2}\big(v_\mathrm{L}^\mathrm{amp}\big)^2 \bar{\bar{u}}_1(k)\,, \tag{48}$$

with

$$\bar{\bar{u}}_0 = \begin{bmatrix} 1 \\ 0 \\ 0 \\ 1 \end{bmatrix}, \quad \bar{\bar{u}}_1(k) = \begin{bmatrix} -\cos(2k\omega\Delta t) \\ \sin(2k\omega\Delta t) \\ \sin(2k\omega\Delta t) \\ \cos(2k\omega\Delta t) \end{bmatrix}. \tag{49}$$

According to superposition principle of linear systems, the particular solution of (37) is the sum of particular solution $\bar{\bar{Y}}_0$ to $\bar{\bar{U}}_0$ and particular solution $\bar{\bar{Y}}_1(k)$ to $\bar{\bar{U}}_1(k)$. Moreover, for $\bar{\bar{U}}_0$, (37) implies

$$\bar{\bar{Y}}_0 = \big(v_\mathrm{L}^\mathrm{amp}\big)^2 \bar{\bar{M}}_0(\omega)\,, \tag{50}$$

with

$$\bar{\bar{M}}_0(\omega) = \frac{1}{2}\bar{\bar{\mathbf{C}}}(\bar{\bar{\mathbf{I}}} - \bar{\bar{\mathbf{A}}})^{-1}\bar{\bar{\mathbf{B}}}\bar{\bar{u}}_0\,. \tag{51}$$

For $\bar{\bar{U}}_1(k)$, the Z-transform of (37) yields the transfer function matrix

$$\begin{aligned} \bar{\bar{\Gamma}}(z) &:= [\bar{\bar{\gamma}}_1(z) \quad \bar{\bar{\gamma}}_2(z) \quad \bar{\bar{\gamma}}_3(z) \quad \bar{\bar{\gamma}}_4(z)] \\ &= \bar{\bar{\mathbf{C}}}(z\bar{\bar{\mathbf{I}}} - \bar{\bar{\mathbf{A}}})^{-1}\bar{\bar{\mathbf{B}}}. \end{aligned} \tag{52}$$

Similar to the mean dynamics analysis, one can obtain steady state output to the harmonic excitations by applying superposition principle and trigonometric identities, yielding

$$\bar{\bar{Y}}_1(k) = \big(v_\mathrm{L}^\mathrm{amp}\big)^2 \bar{\bar{M}}_1(\omega)\sin(2k\omega\Delta t + \bar{\bar{\psi}}(\omega)), \tag{53}$$

where

$$\bar{\bar{M}}_1(\omega) = \frac{1}{2}\Big(\big(\mathrm{Re}(\bar{\bar{\gamma}}_4 - \bar{\bar{\gamma}}_1) + \mathrm{Im}(\bar{\bar{\gamma}}_2 + \bar{\bar{\gamma}}_3)\big)^2 + \big(\mathrm{Im}(\bar{\bar{\gamma}}_1 - \bar{\bar{\gamma}}_4) + \mathrm{Re}(\bar{\bar{\gamma}}_2 + \bar{\bar{\gamma}}_3)\big)^2\Big)^{\frac{1}{2}}, \tag{54}$$

and $\bar{\bar{\psi}}(\omega)$ is the phase lag at frequency ω. Therefore, at steady state, we have

$$\begin{aligned}\bar{\bar{Y}}_{\mathrm{ss}}(k) &= \bar{\bar{Y}}_0 + \bar{\bar{Y}}_1(k) \\ &= \big(v_{\mathrm{L}}^{\mathrm{amp}}\big)^2\Big(\bar{\bar{M}}_0(\omega) + \bar{\bar{M}}_1(\omega)\sin\big(2k\omega\Delta t + \bar{\bar{\psi}}(\omega)\big)\Big).\end{aligned} \tag{55}$$

Recall that $\bar{Y}(k) = \mathbb{E}[\tilde{v}(k)] \in \mathbb{R}$ and $\bar{\bar{Y}}(k) = \mathbb{E}[\tilde{v}^2(k)] - \mathbb{E}[\tilde{v}(k)]^2 \in \mathbb{R}$. Define

$$\mu = \bar{Y}_{\mathrm{ss}}(k)\,, \quad \sigma^2 = \bar{\bar{Y}}_{\mathrm{ss}}(k)\,, \tag{56}$$

that are the mean and variance of $\tilde{v}(k)$ at steady state. Note that the variance $\bar{\bar{Y}}_{\mathrm{ss}}(k)$ is non-negative. Thus, (55) implies that $\bar{\bar{M}}_0(\omega) \geq \bar{\bar{M}}_1(\omega)$. From Chebyshev's inequality [16], we know that the probability of $\tilde{v}(k)$ being outside the $n\sigma$ window $[\mu - n\sigma, \mu + n\sigma]$, $n \in \mathbb{R}^+$ is rather small. Therefore, using (43,55), we can calculate

$$\begin{aligned}\mu \pm n\sigma = v_{\mathrm{L}}^{\mathrm{amp}}\Big[&\bar{M}(\omega)\sin(k\omega\Delta t + \bar{\psi}(\omega)) \\ &\pm n\sqrt{\bar{\bar{M}}_0(\omega) + \bar{\bar{M}}_1(\omega)\sin\big(2k\omega\Delta t + \bar{\bar{\psi}}(\omega)\big)}\Big],\end{aligned} \tag{57}$$

which is a periodic function with period $T = \frac{2\pi}{\omega\Delta t}$. Thus, the total amplification ratio becomes

$$\begin{aligned}\bar{\bar{M}}(\omega) = \max_{0\leq k\leq T}\Big\{\Big|&\bar{M}(\omega)\sin(k\omega\Delta t + \bar{\psi}(\omega)) \\ &\pm n\sqrt{\bar{\bar{M}}_0(\omega) + \bar{\bar{M}}_1(\omega)\sin\big(2k\omega\Delta t + \bar{\bar{\psi}}(\omega)\big)}\Big|\Big\}.\end{aligned} \tag{58}$$

The system is said to be $n\sigma$ string stable if the amplitude of the input $\tilde{v}_{\mathrm{L}}(k)$ is attenuated such that $|\mu \pm n\sigma| < v_{\mathrm{L}}^{\mathrm{amp}}$, i.e., the oscillations are constrained in the interval $[\mu - n\sigma, \mu + n\sigma]$. Henceforth, the necessary and sufficient condition for $n\sigma$ string stability is given by

$$\bar{\bar{M}}(\omega) < 1\,. \tag{59}$$

In Fig. 3, the string stability boundaries are plotted in the $(K_{\mathrm{v}}, K_{\mathrm{p}})$-plane as solid green and blue curves for different values of the packet delivery ratio q and sampling time Δt. For the mean dynamics, the critical frequency is zero along the straight lines given by (46) while $\bar{\omega}_{\mathrm{cr}} > 0$ along the curve given by (45). The union of light green and light blue shaded regions correspond to mean string stable regions, while the light blue shaded region represents the 1σ string stable region. These are embedded in the plant stable regions. We remark that there are some other string stability boundaries outside the plant stable domain which are not shown here. The mean and $n\sigma$ string stable domains shrink when packet delivery ratio q decreases or the sampling time Δt increases. When exceeding critical values, the domains disappear, in which case there exist no gain combinations that can maintain string stability.

VIII. Conclusions

In this paper, the effects of stochastic delays on the dynamics of connected vehicles were studied by analyzing both the mean and covariance dynamics. Necessary and sufficient plant and string stability conditions were derived and it was shown that the stability domains shrink when the packet drop ratio or the sampling time increases. Above a critical limit string stability cannot be achieved by any gain combinations. Our future research include the application of the developed mathematical tools to large vehicular systems with more complicated connectivity structure.

ACKNOWLEDGMENT

This work was supported by NSF grant 1300319. We also thank Mehdi Sadeghpour for helpful discussions.

References

[1] G. Orosz, "Connected cruise control: modeling, delay effects, and nonlinear behavior," *Vehicle System Dynamics*, 2014, submitted.

[2] J. I. Ge, S. S. Avedisov, and G. Orosz, "Stability of connected vehicle platoons with delayed acceleration feedback," in *Proceedings of the ASME Dynamical Systems and Control Conference*, no. DSCC2013-4040. ASME, 2013, p. V002T30A006.

[3] L. Zhang and G. Orosz, "Designing network motifs in connected vehicle systems: delay effects and stability," in *Proceedings of the ASME Dynamical Systems and Control Conference*, no. DSCC2013-4081. ASME, 2013, p. V003T42A006.

[4] D. Caveney, "Cooperative vehicular safety applications," *IEEE Control Systems Magazine*, vol. 30, no. 4, pp. 38–53, 2010.

[5] W. B. Qin and G. Orosz, "Digital effects and delays in connected vehicles: Linear stability and simulations," in *Proceedings of the ASME Dynamical Systems and Control Conference*, no. DSCC2013-3830. ASME, 2013, p. V002T30A001.

[6] F. Bai and H. Krishnan, "Reliability analysis of DSRC wireless communication for vehicle safety applications," in *Proceedings of the IEEE Intelligent Transportation Systems Conference*. IEEE, 2006.

[7] A. Laub, *Matrix Analysis for Scientists and Engineers*. the Society for Industrial and Applied Mathematics, 2005.

[8] G. J. L. Naus, R. P. A. Vugts, J. Ploeg, M. R. J. G. van de Molengraft, and M. Steinbuch, "String-stable CACC design and experimental validation: A frequency-domain approach," *IEEE Transactions on Vehiclular Technology*, vol. 59, no. 9, pp. 429–436, 2010.

[9] K. Lidström, K. Sjöberg, U. Holmberg, J. Andersson, F. Bergh, M. Bjäde, and S. Mak, "A modular CACC system integration and design," *IEEE Transactions on Intelligent Transportation System*, vol. 13, no. 3, pp. 1050–1061, 2012.

[10] M. R. I. Nieuwenhuijze, T. van Keulen, S. Öncü, B. Bonsen, and H. Nijmeijer, "Cooperative driving with a heavy-duty truck in mixed traffic: Experimental results," *IEEE Transactions on Intelligent Transportation System*, vol. 13, no. 3, pp. 1026–1032, 2012.

[11] J. Ploeg, D. P. Shukla, N. van de Wouw, and H. Nijmeijer, "Controller synthesis for string stability of vehicle platoons," *IEEE Transactions on Intelligent Transportation System*, vol. 15, no. 2, pp. 854–865, 2014.

[12] M. Wang, W. Daamen, S. P. Hoogendoorn, and B. van Arem, "Rolling horizon control framework for driver assistance systems. part I: Mathematical formulation and non-cooperative systems," *Transportation Research Part C*, 2014.

[13] J. Guckenheimer and P. Holmes, *Nonlinear Oscillations, Dynamical Systems, and Bifurcations of Vector Fields*. Springer-Verlag, 1983, no. 42.

[14] D. Swaroop and J. K. Hedrick, "String stability of interconnected systems," *IEEE Transactions on Automatic Control*, vol. 41, no. 3, pp. 349–357, 1996.

[15] W. B. Qin, M. M. Gomez, and G. Orosz, "Stability analysis of connected cruise control with stochastic delays," in *Proceedings of American Control Conference*, 2014, pp. 4624 – 4629.

[16] W. Feller, *An Introduction to Probability Theory and Its Applications*. John Wiley & Sons, Inc., 1950, vol. 1.